PNAS RESEARCH ARTICLE | CELL BIOLOGY

Condition-specific 3′ mRNA isoform half-lives and stability elements in yeast

Joseph V. Geisberg[a,1], Zarmik Moqtaderi[a,1], and Kevin Struhl[a,2]

Contributed by Kevin Struhl; received January 19, 2023; accepted March 31, 2023; reviewed by Joan A. Steitz and Lars M. Steinmetz

Alternative polyadenylation generates numerous 3′ mRNA isoforms that can differ in their stability, structure, and function. These isoforms can be used to map mRNA stabilizing and destabilizing elements within 3′ untranslated regions (3′UTRs). Here, we examine how environmental conditions affect 3′ mRNA isoform turnover and structure in yeast cells on a transcriptome scale. Isoform stability broadly increases when cells grow more slowly, with relative half-lives of most isoforms being well correlated across multiple conditions. Surprisingly, dimethyl sulfate probing reveals that individual 3′ isoforms have similar structures across different conditions, in contrast to the extensive structural differences that can exist between closely related isoforms in an individual condition. Unexpectedly, most mRNA stabilizing and destabilizing elements function only in a single growth condition. The genes associated with some classes of condition-specific stability elements are enriched for different functional categories, suggesting that regulated mRNA stability might contribute to adaptation to different growth environments. Condition-specific stability elements do not result in corresponding condition-specific changes in steady-state mRNA isoform levels. This observation is consistent with a compensatory mechanism between polyadenylation and stability, and it suggests that condition-specific mRNA stability elements might largely reflect condition-specific regulation of mRNA 3′ end formation.

mRNA stability elements | regulated mRNA turnover | polyadenylation | mRNA 3′ end formation | yeast

Significance

Alternative polyadenylation generates numerous 3′ mRNA isoforms that can differ in stability, structure, and function, with differential isoform stability mediated by sequence elements within 3′ untranslated regions. We identify >1,000 yeast mRNA stabilizing and destabilizing elements that function in only one of four growth conditions tested. Genes associated with some classes of these condition-specific stability elements are enriched for specific functional categories. Surprisingly, individual 3′ isoforms have similar structures across different conditions. Condition-specific stability elements do not yield corresponding condition-specific changes in steady-state mRNA isoform levels. These observations suggest that, in yeast, regulated mRNA stability might facilitate adaptation to different growth environments and that condition-specific mRNA stability elements might reflect condition-specific regulation of mRNA 3′ end formation.

Eukaryotic cells respond to environmental conditions via transcriptional and posttranscriptional reprogramming. Cells adapt to external stress or changes in growth conditions by coordinately inducing and/or repressing transcription to alter the levels of hundreds, and perhaps thousands, of mRNAs. The yeast *Saccharomyces cerevisiae* undergoes a general transcriptional response to many kinds of stress, but also exhibits condition-specific responses to individual environmental perturbations (1, 2). In different yeast species, transcriptional responses to a given condition are quite different on an individual gene level, but compensatory changes among related genes contribute to similar physiological responses (3).

Expression of a typical eukaryotic gene gives rise to numerous mRNA isoforms that can differ at the 5′ and/or 3′ termini as well as in the inclusion or absence of exons. mRNA isoforms from the same gene can be regulated in response to environmental or developmental cues via alternative promoters (4, 5), polyadenylation sites (6), and mRNA splicing (7, 8). Cancer cells and pluripotent stem cells preferentially express shorter 3′ mRNA isoforms, whereas differentiated cells preferentially express longer 3′ mRNA isoforms (6). Yeast cells subject to diauxic conditions preferentially express shorter 3′ isoforms via a mechanism that links alternative polyadenylation to the speed of transcriptional elongation (9). In contrast, there is limited information on regulation of mRNA isoform stability, structure, and function, particularly at the transcriptome scale.

In *S. cerevisiae* and other yeast species, a typical gene yields ~50 3′ mRNA isoforms arising from different polyadenylation sites in its 3′ untranslated region (3′ UTR) (10–12). Such 3′ mRNA isoforms, even those differing by one or a few nucleotides, can differ dramatically with respect to mRNA stability, structure throughout the 3′UTR, and association with Pab1, the poly(A)-binding protein (13, 14). Sequences responsible for isoform-specific structures, differential Pab1 binding, and mRNA stability are evolutionarily conserved, indicating biological function (14). In mammalian cells, sequences within 3′ UTRs can affect isoform half-life, transcript localization, structure, and translation, and they can also act as a scaffold for macromolecular complexes (15, 16).

Based on clusters of same-gene mRNA isoforms with different half-lives, we identified sequence elements conferring mRNA stabilization or destabilization in yeast cells (13). These mRNA stabilizing and destabilizing elements are abundant (>30% of all genes possess at least one such element), and some elements can affect the turnover rate of a transcript by more than fivefold (13). Double-stranded structures at or near 3′ ends,

Author contributions: J.V.G., Z.M., and K.S. designed research; J.V.G. and Z.M. performed research; J.V.G. contributed new reagents/analytic tools; J.V.G., Z.M., and K.S. analyzed data; and J.V.G., Z.M., and K.S. wrote the paper.

Reviewers: J.A.S., Yale University; and L.M.S., European Molecular Biology Laboratory.

The authors declare no competing interest.

[1]J.V.G. and Z.M. contributed equally to this work.

[2]To whom correspondence may be addressed. Email: kevin@hms.harvard.edu.

This article contains supporting information online at https://www.pnas.org/lookup/suppl/doi:10.1073/pnas.2301117120/-/DCSupplemental.

Published April 24, 2023.

including those mediated by the poly(A) tail and U-rich sequences in 3′UTRs, are a major determinant of mRNA stability (13). Stability elements are often associated with altered structures mediated in large part by interactions with mRNA-binding proteins that recognize specific sequences or structures (14).

There is limited information about how environmental conditions affect individual 3′ mRNA isoform half-lives and mRNA stability elements. Here, we survey the global landscape of 3′ mRNA isoform half-lives, mRNA stability elements within 3′ UTRs, and 3′ mRNA isoform structure in yeast cells grown in multiple conditions. Surprisingly, we find that most of the >1,000 identified mRNA stabilizing and destabilizing elements within 3′UTRs function in a single growth condition. We also determine that structures of the affected 3′ mRNA isoforms are similar under various conditions. Some classes of condition-specific stability elements are enriched for genes in distinct functional categories, suggesting that condition-specific isoform turnover may contribute to adaptation to changing growth environments.

Results

Determining 3′ mRNA Isoform Half-Lives under Multiple Conditions. We previously measured the half-lives of > 20,000 3′ mRNA isoforms originating from thousands of genes in yeast cells grown in YPD medium (13). This was accomplished by rapidly depleting Rpb1, the catalytic subunit of RNA polymerase II (Pol II), from the nucleus by the anchor-away method (17), followed by measuring the relative levels of the 3′ isoforms at multiple time points after the Pol II shutoff. Here, we analyze the same type of data from cells grown in four conditions: rich medium ("YPD"), rich medium with galactose as the carbon source ("YPGal"), rich medium containing sorbitol to cause osmotic stress ("Sorbitol"), and minimal medium containing glucose ("Minimal"). We obtained half-lives for ~ 17,000 to 29,000 3′ isoforms, representing 3,575 to 4,509 genes per condition. Biological replicates are well correlated at the isoform and gene levels (*SI Appendix*, Fig. S1*A*), and isoform half-lives in YPD are well correlated with previous measurements (13) using a different method to map poly(A) sites (*SI Appendix*, Fig. S1*B*).

Half-lives of 3′ mRNA isoforms range over two orders of magnitude (Fig. 1*A* and *SI Appendix*, Table S1). For isoforms present in all four conditions at levels sufficient for half-life analysis, median 3′ isoform stabilities in Minimal (38 min) and Sorbitol (22 min) are greater than in YPD (18 min), broadly in line with the longer doubling times (Minimal, 130 min; Sorbitol, 100 min; YPD, 90 min) as expected from the usual link between rates of cell growth and biological processes. Similarly, median mRNA half-lives per gene in Minimal and Sorbitol are considerably longer than in YPD (*SI Appendix*, Fig. S1*C*). In contrast, gene- and isoform-level mRNA turnover rates are similar in YPGal and YPD, even though the strain grows significantly more slowly in YPGal (the doubling time is 130 min). It is unknown why half-lives in YPGal are shorter than expected from the growth rate, but it might be related to the observation that steady-state mRNA levels in YPGal are ~fivefold lower than in YPD (18).

Relative Half-Lives of 3′ mRNA Isoforms and Their Gene-Specific Variability Are Strongly Correlated across Conditions. Pairwise same-isoform half-life correlations across the four conditions are

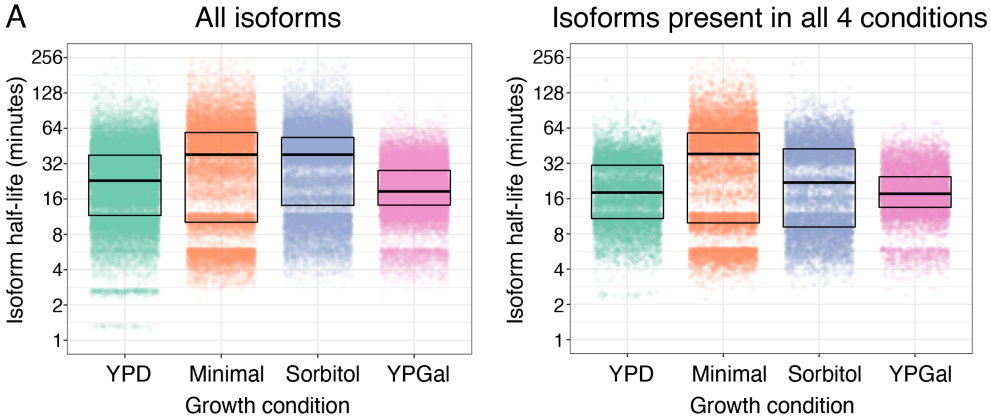

B

	YPD	Minimal	Sorbitol	YPGal
YPD		0.69	0.74	0.60
Minimal	0.69		0.78	0.58
Sorbitol	0.74	0.78		0.51
YPGal	0.60	0.58	0.51	

Fig. 1. 3′ mRNA isoform half-lives under different growth conditions. (*A*) Half-lives (in minutes; $\log_2$ scale) of individual isoforms (each isoform represented by a dot) in the indicated growth condition. Results shown for all isoforms in an individual condition (*Left*) or present in all four conditions (*Right*). The box indicates isoforms between the 25th and 75th percentiles, and the horizontal line represents the median half-life. (*B*) Pairwise correlations between 3′ isoform half-lives in two conditions.

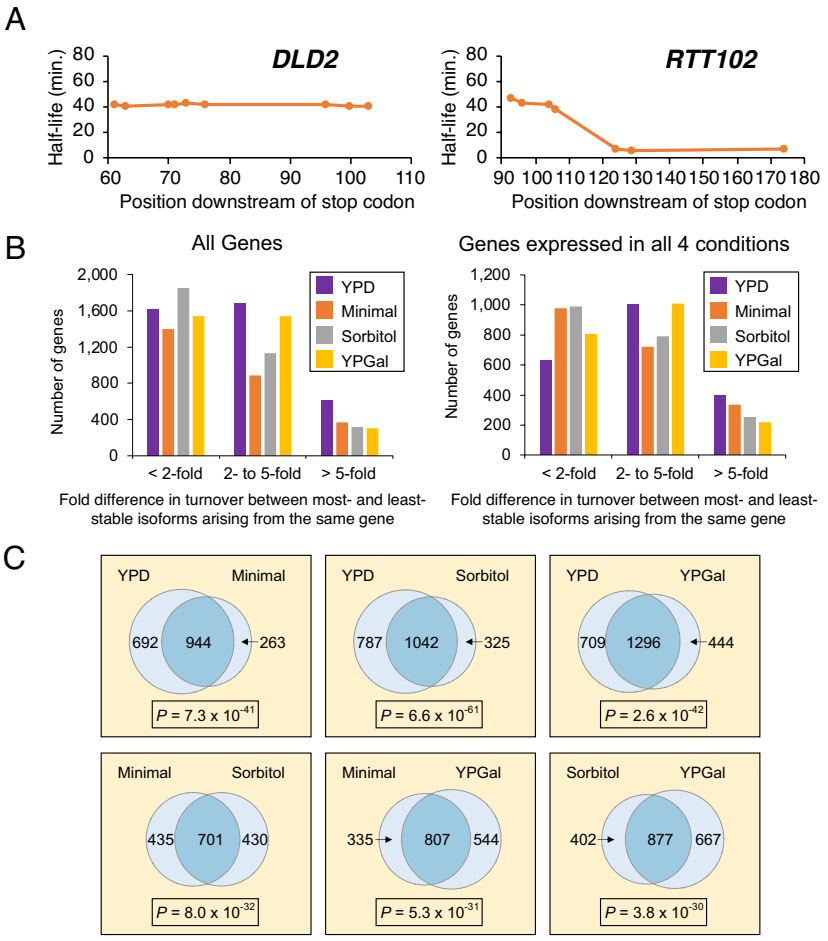

Fig. 2. Half-life variation among isoforms within individual genes. (*A*) Relative half-lives (log_2 scale) of the indicated 3′ isoforms from genes that do not (*Left*) or do (*Right*) show half-life variation in YPD. Half-lives are calculated from the slopes of the decay curves. (*B*) Number of genes having the indicated fold-difference between the most stable and least stable isoform of each individual gene. Results shown for all isoforms in an individual condition (*Left*) or present in all four conditions (*Right*). (*C*) Venn diagrams showing the overlap of individual genes showing more than a twofold difference between their most and least stable isoforms in the indicated growth conditions. For each pairwise comparison, the significance of the overlap (*P* values) calculated by the hypergeometric test is indicated in boxes.

generally high (R = 0.51 to 0.78), indicating that environmental changes affect the turnover of most isoforms (Fig. 1*B*) or genes (*SI Appendix*, Fig. S1*D*) to a similar degree. In each of the four conditions, roughly half the genes (range 44 to 59%) have 3′ isoforms that exhibit greater than twofold half-life differences (Fig. 2 *A* and *B* and *SI Appendix*, Fig. S2*A*). Of note, 9 to 16% of genes (> 300 genes/condition) exhibit high (greater than fivefold) 3′ isoform half-life variation in each of the four conditions. The genes with isoform stability variation in YPD identified here and in a previous study using different methodology (13) exhibit a very high degree (~80%; $P = 2 \times 10^{-34}$, hypergeometric test) of overlap (*SI Appendix*, Fig. S2*B*). Furthermore, genes exhibiting greater than twofold variation in isoform turnover highly overlap in all four conditions (Fig. 2*C*). These results indicate that variability of 3′ mRNA isoform stability is an inherent gene-specific feature that is largely independent of environmental condition.

Structures of 3′ mRNA Isoforms Are Similar across Conditions. Previously, we used DREADS, a dimethyl sulfate (DMS)-based assay, to examine the structures of individual 3′ mRNA isoforms in vivo on a transcriptome scale (14). DMS reactivity is influenced by both RNA structure per se and RNA-protein interactions, so DREADS-based structures do not distinguish between these two aspects of isoform structure. In cells grown in YPD medium, there are many examples of 3′ isoforms that overlap almost completely in sequence yet have dramatically different DMS reactivity profiles (R < 0.3) and hence structures throughout the 3′ UTR (14). As observed previously in YPD (14), pairs of mRNA isoforms with greater differences in stability also show higher structural divergence in all conditions (*SI Appendix*, Fig. S3).

In contrast, the distribution of Pearson correlation coefficients of DMS reactivity profiles for any pair of conditions is very similar to those of biological replicates (Fig. 3). Few mRNA isoforms exhibit strong differences in DMS reactivity profiles (correlation < 0.4), although there may be modest differences (correlations 0.4 to 0.6) in a very small number of isoforms between cells grown in YPGal compared to other conditions. Thus, on a genome-wide scale, 3′ mRNA isoform structures are similar across all conditions.

Identification of 3′ mRNA Isoforms with Condition-Specific Half-Lives. For each isoform, we first normalized half-lives in each condition relative to the median stability values in each condition and then compared the normalized half-lives under all four conditions. To identify isoforms having a condition-specific half-life, we required that 1) the isoform have a > 1.5-fold shorter or longer normalized half-life in one condition as compared to each of the other three conditions, and 2) the normalized isoform half-lives in the three other conditions all be within a span of no greater than 1.5-fold. By this definition, we identified 1,392 isoforms

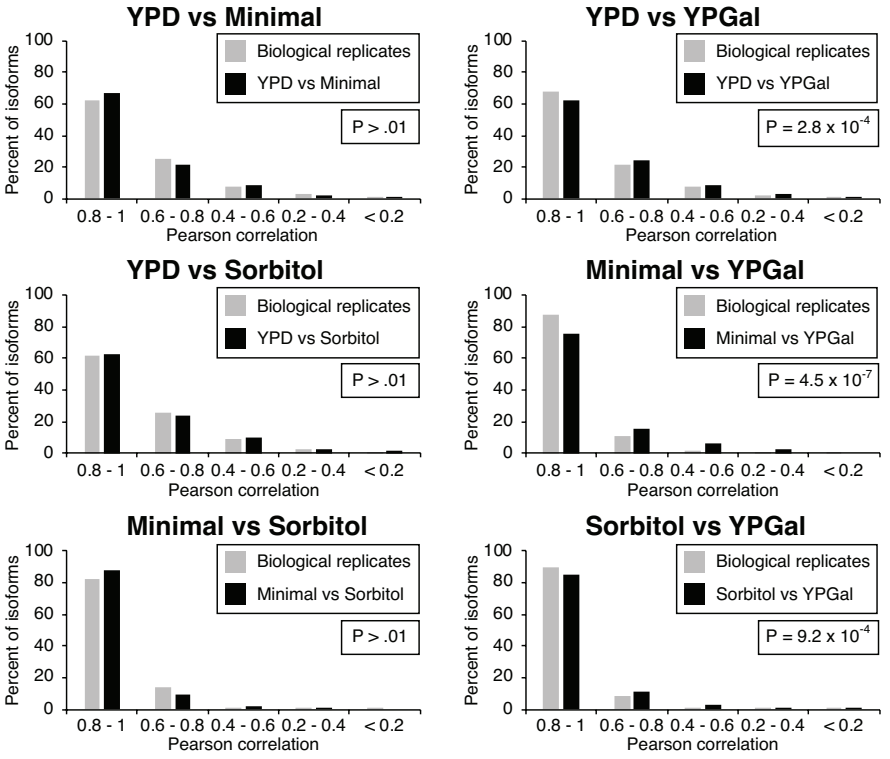

Fig. 3. DREADS-based structures of 3′ mRNA isoforms in various growth conditions. Frequency distribution of biological replicates (gray bars) and pairwise comparisons (black bars) with the indicated ranges of Pearson correlation coefficients.

with condition-specific half-lives (Fig. 4*A*). Of these, 456 isoforms were conditionally stabilized and 936 isoforms were conditionally destabilized. Using a more stringent cutoff of a twofold difference in stability revealed 444 isoforms with condition-specific half-lives; a threefold cutoff identified 75 such isoforms. mRNA decay curves for isoforms with similar half-lives across conditions are shown in

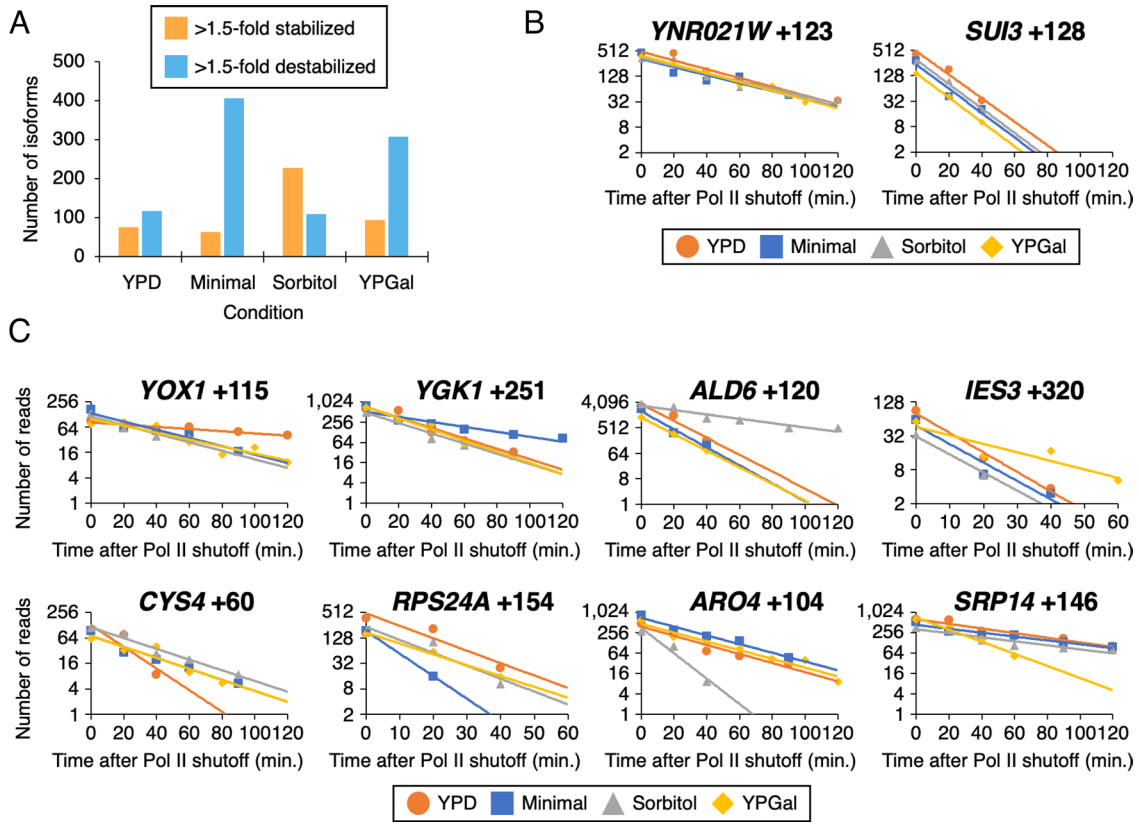

Fig. 4. Isoforms with condition-specific half-lives. (*A*) Number of isoforms with condition-specific half-lives. There are eight classes of isoforms that are defined by whether the isoform is stabilized or destabilized under the indicated condition. (*B*) mRNA decay curves for isoforms with similar half-lives across conditions. RNA levels at each time point after Pol II sequestration are plotted for YPD (orange), Minimal (blue), Sorbitol (gray), and YPGal (gold). Isoform half-lives in each condition are calculated from the slopes of the decay curves. (*C*) mRNA decay curves for the 8 classes of isoforms with condition-specific half-lives. For each isoform, RNA levels at each time point after Pol II inactivation are plotted under the four conditions indicated by different colors. Half-lives are calculated from the slopes of the decay curves.

Fig. 4*A*, and examples of the eight classes of isoforms (stabilized or destabilized in the four conditions) with condition-specific half-lives are shown in Fig. 4*B*.

Identification of mRNA Stability Elements under Different Conditions. We previously identified sequence elements conferring mRNA stabilization or destabilization based on the properties of clusters of 3′ mRNA isoforms sharing closely spaced 3′ termini and similar half-lives (13). Here, we define an mRNA stability element more simply as the sequence between the endpoints of two consecutive 3′ isoforms that have different half-lives (Fig. 5*A*). A stabilizing element is one for which the longer isoform (ending downstream of, and thus containing, the element) is more stable than the shorter isoform ending upstream of the element. Conversely, a destabilizing element is one for which the adjacent downstream-ending isoform is less stable than the upstream-ending isoform. Regions between neighboring isoform endpoints have similar size ranges (median of 4 nt) and turnover distributions in all four conditions (*SI Appendix*, Fig. S4 *A* and *B*). For each condition, most regions between neighboring isoform endpoints (88 to 93%) have little or no effect on the isoforms' relative turnover rates, and the downstream:upstream isoform half-life ratio distributions are similar (Fig. 5*B*). However, ~10% of all neighboring isoforms have at least a twofold increased or decreased half-life of the longer isoform, with destabilizing elements (red bars) slightly outnumbering stabilizing elements (green bars). In all four conditions, destabilizing and stabilizing elements are longer than neutral inter-isoform regions that do not affect isoform turnover (Fig. 5*B*, blue lines). These additional sequences in destabilizing and stabilizing elements within 3′UTRs, although small with respect to overall mRNA length, could encode protein-binding sites and/or other motifs of functional significance.

Identification of Condition-Specific mRNA Stability Elements by Hierarchical Clustering. We used several approaches to identify mRNA stabilizing or destabilizing elements that function in a condition-specific manner. For these analyses, individual isoforms must have sufficient steady-state levels under all conditions for half-lives to be reliably measured and compared. Gene-specific expression changes and statistical variation of steady-state expression levels among modestly expressed mRNA isoforms limit the number of isoforms that can be analyzed. Thus, many mRNA stabilizing and destabilizing elements observed in one condition cannot be analyzed in other conditions.

We first performed hierarchical clustering to classify sequence regions between neighboring isoform endpoints. Using relative stability of the flanking mRNA isoforms ($\log_2$ distal/proximal isoform half-life) as the sole input, we categorized these sequence regions into groups whose members share a similar profile in how they affect stability in the various growth conditions. Hierarchical clustering was restricted to the 3,532 regions between neighboring isoform ends with high enough steady-state expression levels and measurable half-lives under all conditions (*SI Appendix*, Fig. S4*C* and Dataset S1). We settled on 12 as the optimal number of groups (clusters), as higher numbers predominantly add groups with very few (1 to 5) members.

More than half of all isoform pairs have similar stability ratios in all conditions, indicating a minimal effect on turnover in any

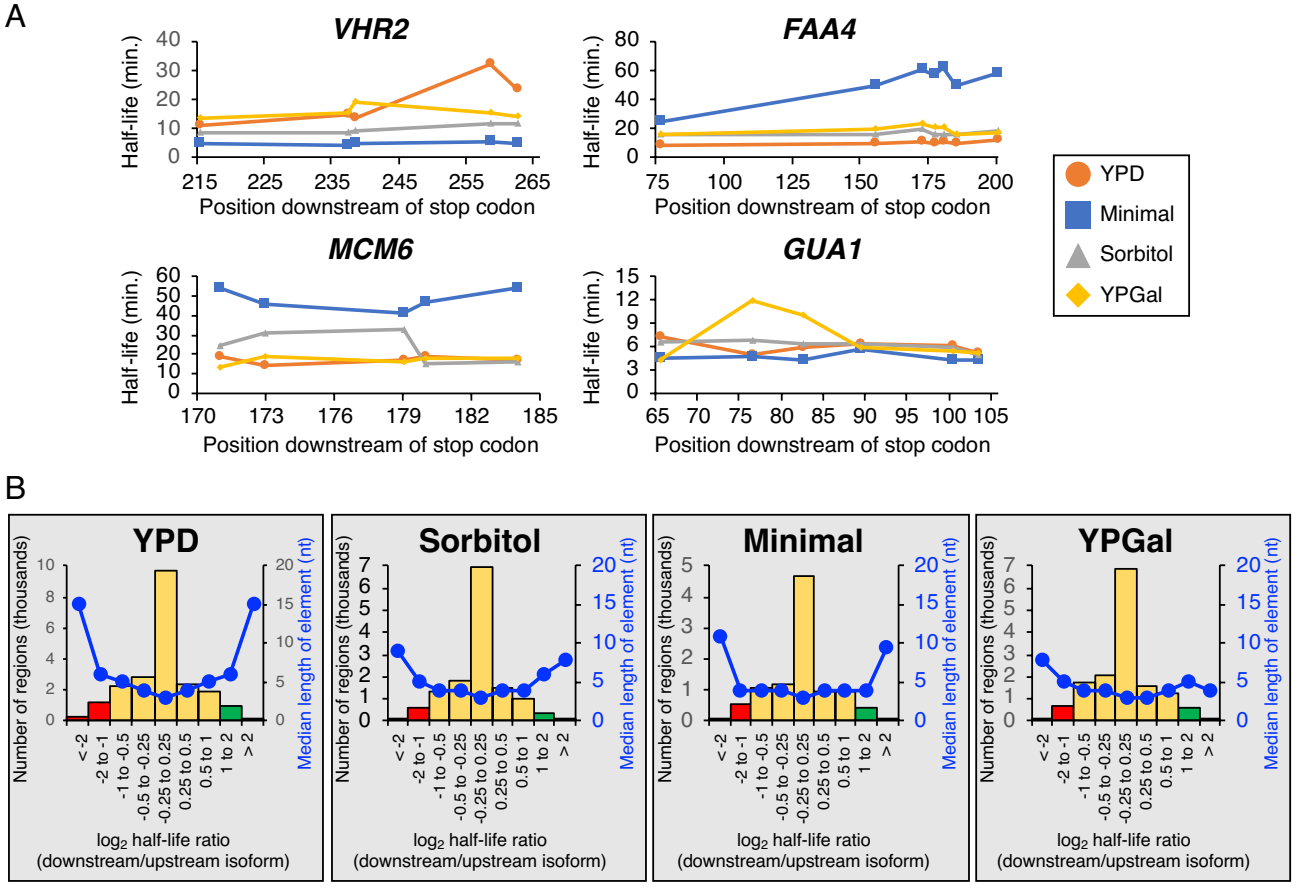

Fig. 5. Identification of mRNA stability elements under different conditions. (*A*) Schematic showing how mRNA stabilizing or destabilizing elements are defined by different half-lives of neighboring isoforms. The region between such isoforms contains or is part of the element, but the extent of the element is not determined. (*B*) For each condition, the number (in thousands; vertical bars) and median length (blue dots and lines) of neighboring 3′ isoform pairs (regions) with the indicated ranges of downstream:upstream half-life ratios ($\log_2$) are shown. Stabilizing (green bars) and destabilizing (red bars) elements are indicated.

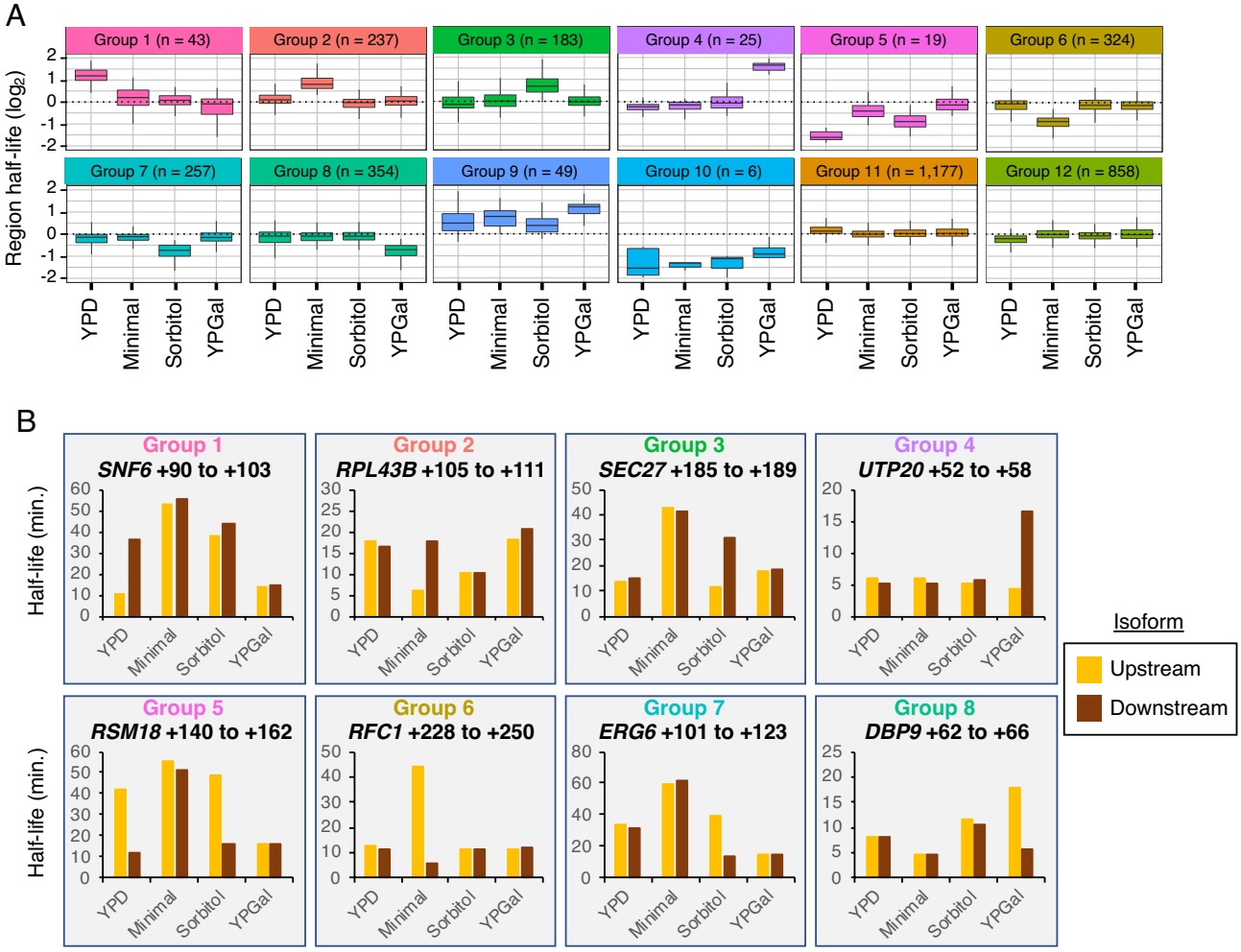

Fig. 6. Identification of condition-specific mRNA stability elements by hierarchical clustering. (*A*) For each of the 12 groups, boxplots of the downstream:upstream half-life ratios (log_2) of the neighboring isoform pairs flanking the regions are shown under the indicated four growth conditions. Condition-specific stabilizing elements have log_2 ratios around +1 in one condition, whereas condition-specific destabilizing elements have log_2 ratios around −1 in one condition. Most regions lack such elements and have log_2 ratios around 0 in all conditions (groups 11 and 12). (*B*) Examples of condition-specific stability elements. For each group, the half-lives of upstream (orange) and downstream (brown) isoforms that define the example element are shown for all four conditions.

condition (groups 11 and 12; Fig. 6*A*). However, the 1,442 (40%) neighboring isoform pairs within groups 1 to 8 exhibit differential mRNA stability in just one (or two, for group 5) of the four conditions, indicating that the regions between their endpoints represent condition-specific mRNA stability elements (Fig. 6*A*). Remarkably, single-condition stabilizing elements are present in all four conditions (groups 1 to 4), while single-condition destabilizing elements are found in 3 of 4 conditions tested (groups 6 to 8). Examples of such condition-specific elements (groups 1 to 8) are shown in Fig. 6*B*. The number of condition-specific stability elements in a group varies between 19 (group 5) and 354 (group 8). Surprisingly, very few (< 2%) of all inter-isoform regions are generally stabilizing (group 9, 49 cases) or generally destabilizing (group 10, 6 cases) in all four conditions (Fig. 6*A*).

For each group consisting of condition-specific stability elements, the number of stability elements is higher (2 to 43% depending on the group) than the number of genes (*SI Appendix*, Table S2). This indicates that although most genes have only one condition-specific stability element, some genes have multiple elements of the same type. Overall, the 1,442 condition-specific elements map to 738 genes, indicating that more than half of all yeast genes in our dataset (67%; 738 out of 1,102 possible genes) contain elements that selectively affect mRNA turnover in a condition-specific manner. By contrast, relatively few genes (53; 5% of all genes analyzed) contain elements that significantly affect turnover in all four conditions.

Condition-Specific mRNA Stability Elements Identified by a Cutoff Approach. For independent corroboration of the above hierarchical clustering results, we analyzed the same 3,532 neighboring isoform pairs using an arbitrary cutoff of 1.5-fold for an inter-isoform region to qualify as stabilizing or destabilizing (i.e., ≥0.5-fold stabilization or destabilization; *SI Appendix*, Fig. S5*A*). By this definition, 1,138 (32%) of the neighboring isoforms (representing 612 genes or 56% of the total) flank a stability element that stabilizes or destabilizes mRNA by ≥ 1.5-fold, a result roughly comparable to the number of stability elements in clusters 1 to 4 and 6 to 8 (1,423 elements; *SI Appendix*, Fig. S5*A*). Most (76%) of these elements function in only one condition, whereas 17% function in two conditions, and 5% function in three conditions (*SI Appendix*, Fig. S5*B*). Only 13 stability elements defined by this cutoff function in all four conditions. As expected, single-condition and all-condition stability elements identified by both approaches strongly overlap (*SI Appendix*, Fig. S6), highlighting the utility of using either approach to identify stability elements. Thus, condition-specific mRNA stability elements occur frequently within yeast 3′ UTRs and vastly outnumber all-condition stability elements.

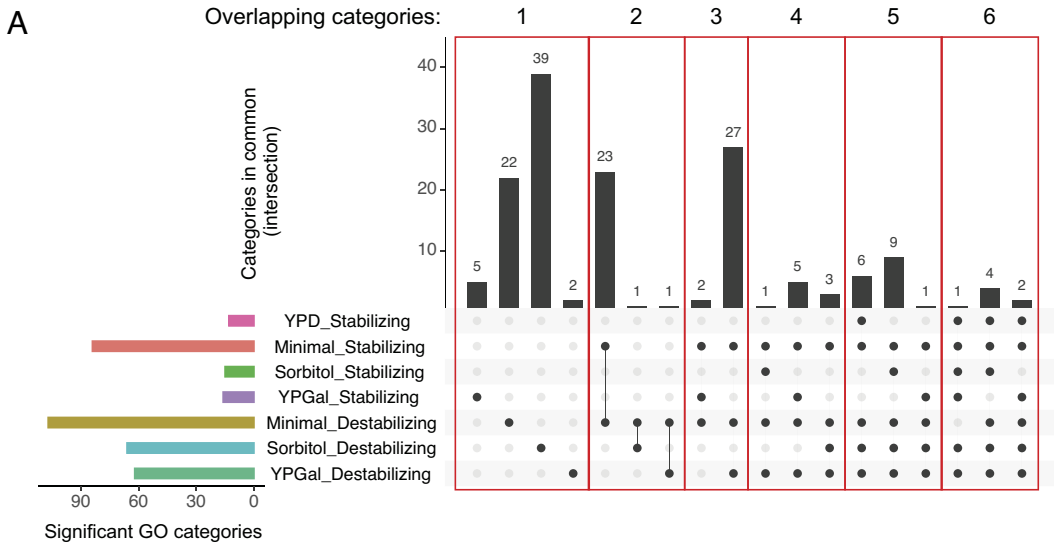

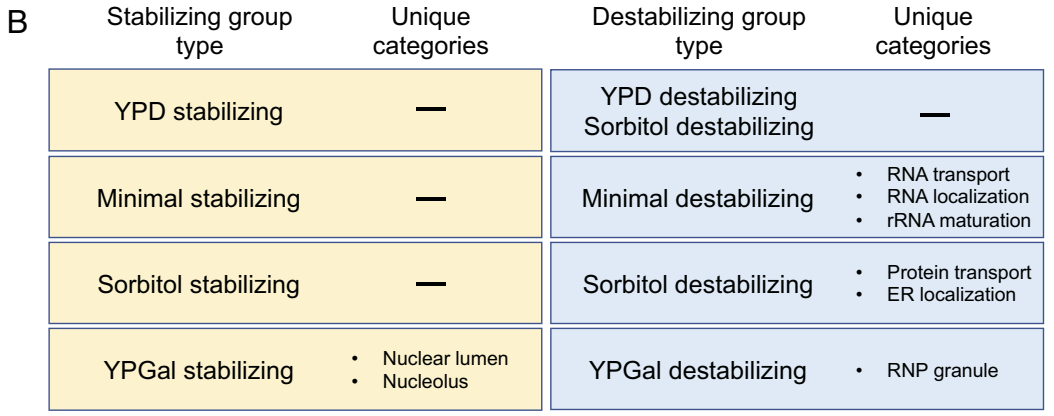

Fig. 7. Condition-specific mRNA stability elements are enriched in different gene categories. (*A*) Number of significant GO categories of overrepresented genes for the indicated classes of condition-specific elements (colored bars, *Left*). Number of GO categories for indicated combinations of condition-specific elements (black dots, *Right*) that are subdivided according to the number of overlapping categories (1 to 6). (*B*) Unique GO categories for the indicated classes of condition-specific stability elements.

Condition-Specific mRNA Stability Elements Identified using Isoform Clusters. As a third approach similar to one that we used previously (13), we examined stability elements between isoform "clusters" (multiple isoforms with closely spaced endpoints, defined here as each no more than 4 nt from the last). Using the summed reads from all isoforms in each cluster, we computed cluster half-lives and then compared the relative turnover rates of consecutive clusters. As there are fewer pairs of neighboring clusters (1,727) than there are pairs of neighboring isoforms (3,532), this approach is more restrictive and may miss potential stability elements. However, the combined read counts of all isoforms within a cluster are higher than read counts of individual isoforms, thereby making half-life measurements more accurate. Of all sequences between the 1,727 neighboring cluster pairs, 651 (38%) show a >1.5-fold stabilizing or destabilizing effect in one condition, whereas only 26 show such effects under all four conditions (*SI Appendix*, Fig. S5*C*). Thus, all three approaches strongly indicate that condition-specific stability elements vastly outnumber elements that function in all conditions.

Condition-Specific mRNA Stability Elements Are Enriched in Different Gene Categories. We used GO enrichment analysis to identify overrepresented gene categories for each group of single-condition mRNA stability elements. To reduce potential artifacts, we required that each condition-specific element within a hierarchical clustering group (except for group 10, which has too few members for this analysis) also possess a > 1.5-fold stability difference within the same condition ("double selection"; *SI Appendix*, Fig. S6). As expected, there is very high overlap between elements identified via hierarchical clustering and those identified by a strict 1.5-fold stability cutoff within individual categories ($P = 4.2 \times 10^{-10}$ to $< 10^{-100}$); the number of elements per double-selected group ranges from 5 to 295. Many overrepresented GO categories are common to multiple groups, and these primarily encode ribosomal protein (RP) genes or other loci involved in translation (Fig. 7*A* and Dataset S2). RP and translation-mediating genes generally have high mRNA expression levels and hence are overrepresented in the data, resulting in selection bias (19).

Interestingly, sequences in several single-condition hierarchical clustering groups are from genes enriched in GO categories that fall within specific functional classes (Figs. 7*B* and *SI Appendix*, Fig. S7). Stabilizing elements functioning in YPGal (group 4) are overrepresented in genes having to do with the nucleolus or nuclear lumen, whereas destabilizing elements functioning in YPGal (group 8) are overrepresented in RNP granule genes. Group 6 (destabilizing in Minimal) members come from genes enriched in multiple GO categories affecting RNA transport and localization, and to a lesser extent rRNA maturation. Group 7 elements (destabilizing in Sorbitol) belong to genes falling into categories that predominantly affect protein transport and localization,

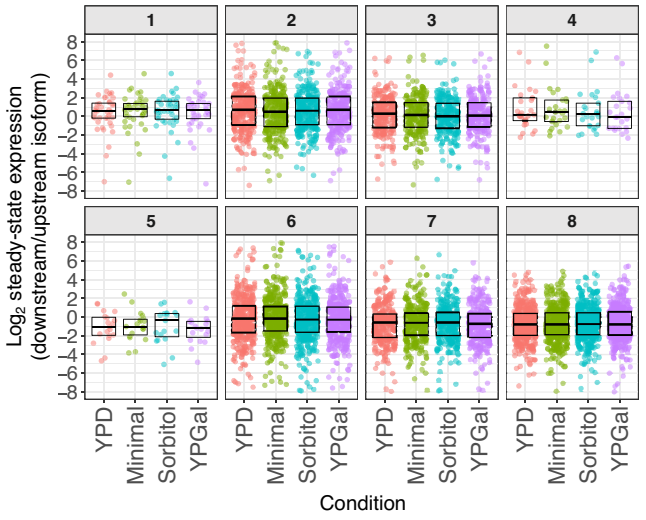

Fig. 8. Steady-state levels of isoforms defining the condition-specific elements are similar across conditions. Boxplots of steady-state expression ratios (log_2) of downstream:upstream isoforms flanking the indicated 8 classes of condition-specific stability elements. Each dot represents an individual condition-specific element. Boxes represent the elements within the 25th to 75th percentiles, and the horizontal line represents the median value.

including to the endoplasmic reticulum (ER). This observation suggests that at least some condition-specific elements are likely to be biologically significant.

Neighboring mRNA Isoforms with Condition-Specific Half-Life Differences Do Not Have Condition-Specific Differences in Steady-State Levels. In previous work, we discovered a compensatory link between polyadenylation in the nucleus and mRNA decay in the cytoplasm (20). Increased efficiency of 3′ end formation at a specific site is associated with reduced stability of the corresponding 3′ mRNA isoform. This inverse relationship between 3′ isoform formation and mRNA isoform half-life occurs in all four conditions tested here (20).

The compensatory link between polyadenylation and mRNA decay could reduce the variability in steady-state levels of mRNA isoforms in response to changes in environmental conditions. To test this idea, we examined steady-state levels of the neighboring isoforms that define the condition-specific elements. Within each of the 8 groups of condition-specific elements, relative RNA levels of the element-defining isoform pairs are similar in all conditions (Fig. 8). Thus, relative steady-state levels of same-gene 3′ mRNA isoforms are maintained even when the stability of some isoforms is altered by environmental conditions.

Discussion

Global vs. Specific Control of mRNA Isoform Half-Lives. In each of the four conditions tested here, half-lives of 3′ mRNA isoforms vary over a 100-fold range, and ~50% of genes express 3′ mRNA isoforms whose half-lives vary by more than twofold. However, relative stabilities of individual 3′ mRNA isoforms are strongly correlated across the four conditions, and there is a strong overlap in genes exhibiting isoform half-life variation. Median 3′ isoform half-lives in Minimal and Sorbitol are greater than in YPD, in accord with longer doubling times and likely reflecting the common linkage between the kinetics of cellular processes and growth rate. In contrast, and for unknown reasons, mRNA turnover rates are similar in YPGal and YPD, even though the strain grows significantly more slowly in YPGal. This discordance between isoform half-lives and growth rate might explain why steady-state mRNA levels in YPGal are approximately fivefold lower than in YPD (18). Thus, yeast cells exert global control of mRNA half-lives, presumably through the mRNA degradation machinery, in response to changing growth environments. Unlike this global control, isoform turnover variation is largely an intrinsic property of a subset of yeast genes.

Most mRNA Stabilizing and Destabilizing Elements Are Condition-Specific. We used three analytical approaches to identify mRNA stabilizing and destabilizing sequence elements and determined that most such elements function in only one of the four growth conditions tested. The three approaches yield a highly overlapping set of elements, indicative of robust results that are not strongly biased by the vagaries of the individual approaches. We identified > 1,000 stability elements, among which are hundreds specific for Sorbitol, Minimal, or YPGal; considerably fewer stability elements are specific for YPD. We were unable to identify common sequence motifs among condition-specific stabilizing or destabilizing elements. This likely reflects the facts that RNA structure plays a key role in RNA–protein interactions and that small structural differences at 3′ isoform termini can engender large structural consequences through the entire 3′UTR, including the actual stability element (14).

Surprisingly, only 1 to 2% of the elements that decrease or increase stability do so in all four conditions. Only 5% of stability elements function in three conditions, whereas 17% function in two conditions. mRNA stability elements effective in YPD often function in another condition(s), explaining the low number of YPD-specific stability elements. Thus, even though relative isoform stability is highly conserved across conditions, mRNA stabilizing and destabilizing elements have a great deal of condition-specificity. These results argue against global upregulation or downregulation of mRNA levels via 3′UTRs and, instead, for the notion that 3′UTRs fine-tune 3′ mRNA isoform half-lives in response to environmental stimuli. In accord with this conclusion, protein-coding sequences, not 3′UTRs, are the primary drivers of overall mRNA stability (21).

Some groups of single-condition stability elements (groups 4, 6, 7, 8) are overrepresented in functionally related GO categories that are absent in other groups. Notably, destabilizing elements specific for Minimal (group 6) or Sorbitol (group 7) are enriched in functional categories that affect localization and transport of either nucleic acids (predominantly RNA; group 6) or proteins/peptides (group 7). In addition, genes containing multiple condition-specific elements of the same type are overrepresented in some groups.

These observations suggest that condition-specific stability elements might serve as an additional layer of biological control. However, condition-specific stability elements do not have corresponding effects on steady-state isoform levels, suggesting that isoform abundance at steady state is not sufficient to explain biological relevance. Instead, condition-specific stability elements may function in modulating the transition between conditions. In this regard, environmental stress responses are typically characterized by a rapid, but transient, induction and/or repression of many transcripts, with most returning to near steady-state levels in 1 to 2 h (1, 2).

Potential Molecular Mechanisms. The mechanisms by which condition-specific mRNA stability elements function are unknown, but several models are possible. In one model, condition-specific differences in abundance and/or activity of RNA-binding proteins might lead to their differential association with stability elements

and subsequent changes in mRNA turnover (22). In apparent contradiction to this model, DMS reactivity profiles, which report on intrinsic RNA structure and interactions with RNA-binding proteins, are largely similar among all the conditions. However, different RNA-binding proteins or different levels or modifications of the same RNA-binding protein could cause subtle or even undetectable structural effects, yet differentially affect turnover. In a related version of this model, condition-specific differences in mRNA modifications (e.g., 6mA, 5mC) around the stability element or other 3′UTR locations could differentially affect turnover, as such posttranscriptional modifications of mRNA are isoform-specific and can alter half-lives (23, 24). This class of models does not easily explain why condition-specific stability elements do not result in condition-specific differences in steady-state isoform levels.

In an alternative model, condition-specific isoform half-lives might arise indirectly from condition-specific differences in the level of cleavage/polyadenylation corresponding to particular 3′ isoforms. In this regard, increased cleavage/polyadenylation in the nucleus at a given site in the 3′UTR is linked to decreased half-life of the corresponding 3′ isoform in the cytoplasm (20). This compensatory mechanism presumably involves a molecular mark [e.g., poly(A) tail length, mRNA modification, or a bound protein] incorporated during (or prior to) the cleavage/polyadenylation process that persists upon translocation from the nucleus to the cytoplasm, whereupon it affects mRNA stability (20). Thus, if environmental conditions affect the efficiency of cleavage/polyadenylation at specific sites, this compensatory mechanism predicts altered isoform half-life with little change in steady-state isoform levels. This class of models could explain the apparent lack of condition-specific differences in isoform structure. Importantly, these two classes of models are not mutually exclusive and indeed may be interdependent.

Materials and Methods

Yeast Strains and Cell Growth. Yeast strain JGY2000 (*MATa, his3Δ0, leu2Δ0, met15Δ0, ura3Δ0, rpb1::RPB1–FRB, rpl13::RPL13–FK512*) contains an anchor-away allele (17) of *RPB1*, which encodes a version of Rpb1 (the largest subunit of Pol II) that permits rapid depletion of Pol II from the nucleus upon treatment with rapamycin (25). Duplicate cultures were grown to early- to mid-log phase in the following conditions (9): YPD broth; YP medium containing 2% galactose (YPGal), osmotic stress (Sorbitol) conditions (YPD + 1M sorbitol); nutrient-poor minimal medium containing 2% dextrose and yeast nitrogen base without amino acids but supplemented with uracil and essential amino acids (Minimal). Cells were then treated with rapamycin to induce Pol II depletion, and time points were taken at 0, 20, 40, 60, 90, and 120 min after rapamycin addition. At each time of harvest, cultures were spiked with 4×10^6 of *S. pombe* cells that served as an internal control to normalize RNA levels among samples.

Measuring 3′ mRNA Isoform Half-Lives. Datasets from Rpb1 depletion time courses used for the half-life analyses have been described previously (20). For measuring levels of 3′ mRNA isoforms, 3′ READS was performed with 25 μg purified total RNA with 18 cycles of amplification as described (26). Barcoded libraries were quantified on an Agilent Bioanalyzer 2100, pooled, and sequenced on the Illumina NextSeq 500 platform. For each growth condition, we normalized 3′ mRNA isoform levels at all time points to the *S. pombe* spike-in control (13).

Half-lives for each isoform (≥30 reads at maximal time point) were calculated essentially as described (13). Briefly, for each isoform, we first identified the time point (either t = 0 or t = 20) containing the maximal number of reads and the time point with a >10-fold drop in sequence reads relative to the maximal time-point. We used these and the values at intervening time points to determine the isoform's half-life by fitting the data using exponential decay curve fitting exactly as described (13). For very stable isoforms whose levels never dropped below the 10-fold threshold relative to maximum level, we used read counts at all time points to compute half-lives. Conversely, we used only two data points to calculate the half-lives of very rapidly decaying transcripts whose read counts dropped > 10-fold (from t = 0 to t = 20 or t = 20 to t = 40). Any isoforms with poor goodness of fit ($R^2 < 0.7$) were eliminated from subsequent analyses. Employing the selection criteria above, the number of isoforms with computable half-lives (using combined biological replicate data) ranges between ~17,000 and 29,000 per condition, with median R^2 values in conditions ranging from 0.88 to 0.93.

Identification of Condition-Specific Stabilized and Destabilized Isoforms. In each condition, half-lives of all in common isoforms were normalized by dividing each isoform's half-life by the median isoform half-life in that condition. To identify condition-specific isoforms, we required 1) that each condition-specific isoform have a > 1.5-fold shorter or longer normalized half-life in one condition as compared to each of the other three conditions, and 2) that the normalized isoform half-lives in the three other conditions all be within a span of no greater than 1.5-fold.

Computation of Cluster- and Gene-level Half-Lives. Cluster half-lives were calculated as follows: First, a list of all unique isoforms that possess ≥ 5 steady-state reads in at least one condition was generated. Same-gene, closely spaced isoforms (≤ 4 nt) were combined into clusters as described (27), and the total number of reads within each cluster was tabulated at all pre-rampamycin and post-rapamycin addition time points. Half-lives for each cluster were computed exactly as for individual isoforms, except that individual isoform read values at each time point were replaced by summed read values over the entire cluster span. Calculation of gene-level half-lives was similar to the method used for clusters and isoforms, except that for all time points, summed read values of all isoforms ending within the first 400 nt downstream of a gene's stop codon were used in place of individual isoform or combined cluster reads.

Cluster-Based Identification of mRNA Stabilizing and Destabilizing Elements. We identified mRNA stabilizing and destabilizing elements by a modification of the adjacent cluster approach (13). Starting with a list of all clusters that possess identical start and end points in the four conditions, we analyzed all consecutive same-gene clusters for which we obtained reliable half-life measurements in all conditions. For each cluster pair, we computed a stability ratio in each of the four conditions by dividing the half-life of the more stable cluster by that of the less stable cluster. Inter-cluster regions with a ≥ 1.5-fold ratio of downstream/upstream cluster half-lives in a given condition were termed stabilizing elements. Conversely, regions with a ≥ 1.5-fold ratio of upstream/downstream cluster half-lives were called destabilizing elements.

Identifying Condition-Specific Stabilizing and Destabilizing Elements by Hierarchical Clustering. We reformatted a list of 3′ isoforms with half-life data in all four conditions into a list of 3,532 interisoform regions (i.e., 3′UTR sequences between two consecutive same-gene isoform endpoints). For each region, we computed the $\log_2$ ratio of the downstream/upstream isoform half-lives in every condition. Distributions of these $\log_2$ half-life ratios were highly similar across conditions, with median values centered on 0 (*SI Appendix*, Fig. S4*C*). We then performed hierarchical clustering on the data in r [relevant code: *hclust*(*dist*(df, method = "minkowski"), method = "complete")], cutting the tree at 12 nodes (groups); additional nodes yielded groups with very few (<5) members.

Condition-Specific Stabilizing and Destabilizing Element Identification Using a Stability Cutoff. For each of the 3,532 interisoform regions, and in each condition, we divided the half-life of the more stable isoform by the half-life of the less stable isoform. If the downstream/upstream 3′ isoform half-life ratio was ≥ 1.5, the region was deemed a stabilizing element in that condition. Conversely, regions for which the ratios of upstream/downstream isoform half-lives exceeded (or were equal to) 1.5-fold were classified as destabilizing elements.

Structural Analysis of 3′ mRNA Isoforms via DREADS. The DREADS procedure for DMS-based structural analysis of 3′ mRNA isoforms has been described previously (14). Cells (15 mL at OD_{600} ~ 0.5) grown in each of the four conditions were supplemented with 4×10^6 *S. pombe* cells as a spike-in control just prior to harvest. Cell cultures were then mock treated (−DMS) or incubated with 500 μL DMS (+DMS) for 2 min at room temperature, quenched twice with 30 mL stop solution (30% beta-mercaptoethanol, 25% isoamyl alcohol), washed with 1 mL H_2O, and frozen at -70 °C. Total RNA was isolated by the hot acid phenol method and purified with RNeasy (Qiagen). Poly(A) mRNA was isolated from 25 μg total RNA via purification with magnetic oligo dT(25) beads (New England Biolabs)

and was then bound to beads precoated with a $U_{45}T_5$-biotinylated mRNA capture oligonucleotide (26). Bead-immobilized mRNA tails were trimmed with RNase H (New England Biolabs) to generate shortened poly(A) sequences averaging ~ 5 As as described (26). After ligation of 5′ preadenylated adapter A to the trimmed mRNA 3′ ends, mRNAs were reverse transcribed with Superscript III (Life Technologies) using primer B (26). cDNAs were ligated with T4 DNA Ligase (NEB) to splint adapter C (24), and the single-stranded DNA products (110 to 500 nt) were purified on 8% polyacrylamide-urea gels. DNA fragments were amplified by 18 cycles of PCR with barcoded oligonucleotides. Amplified libraries were purified with SizeSelector-I beads (Aline Biosciences), quantified via Bioanalyzer 2100 (Agilent Technologies), pooled, and further purified by electrophoresis on 8% polyacrylamide gels. Combined libraries were and paired-end sequenced on the Illumina NextSeq 500 platform.

DREADS Processing Pipeline and Correlation Analysis of 3′ mRNA Isoform Structure. Data from condition-specific demultiplexed −DMS and +DMS libraries were processed as described (24). In brief, paired-end sequencing of each fragment in the DREADS library serves to identify two positions: mapping the read adjacent to the poly(A) tail identifies a unique 3′ isoform, and the corresponding paired read marks the opposite end of the sequenced fragment, giving the position where first-strand cDNA synthesis stopped during library construction. This can occur because of natural factors such as RNA structure, but it can also be indicative of DMS-mediated modification of the adjacent residue. Over the entire sequenced population, all the individual fragments representing a given 3′ isoform will cumulatively yield a distinct pattern of upstream endpoints associated with that isoform. For every isoform, we obtained net DMS reads for each possible upstream position by subtracting the normalized read count in the −DMS control from that of the +DMS sample (setting negative numbers to 0). We refer to this pattern as the DMS reactivity profile of the isoform.

For both replicate and cross-condition analysis (Fig. 3), Pearson correlation coefficients between any two isoform reactivity profiles with a minimum of 1,000 net reads/isoform were computed by correlating position-specific net reads for each isoform over the common window that the two isoforms share. For the analysis of the relationship between half-life variation and structural dissimilarity in neighboring isoform pairs (*SI Appendix*, Fig. S3), we lowered the net reads threshold to ≥ 100 reads/isoform in order to obtain enough members in each bin to perform the analysis.

Data, Materials, and Software Availability. DREADS datasets for the various growth conditions have been deposited in the NCBI Gene Expression Omnibus (GEO) database (28) under accession number GSE228123 (29). The analysis also uses DREADS (14) data from YPD-grown cells previously deposited in GSE95788 (30). Datasets from Rpb1 depletion time courses (20) used for the half-life analysis may be accessed at GSE191091 (31). The comparison with a sequencing method employed in previous work (13) uses data from GSE52286 (32).

ACKNOWLEDGMENTS. We thank Catherine Maddox for excellent technical assistance. This work was supported by grants to K.S. from the NIH (GM 30186 and GM181801).

Author affiliations: [a]Department of Biological Chemistry and Molecular Pharmacology, Harvard Medical School, Boston, MA 02115

1. A. P. Gasch *et al.*, Genomic expression programs in the response of yeast cells to environmental changes. *Mol. Biol. Cell.* **11**, 4241–4257 (2000).
2. H. Taymaz-Nikerel, A. Cankorur-Cetinkaya, B. Kirdar, Genome-wide transcriptional response of Saccharomyces cerevisiae to stress-induced perturbations. *Front. Bioeng. Biotechnol.* **4**, 17 (2016).
3. I. Tirosh, K.-H. Wong, N. Barkai, K. Struhl, Extensive divergence of the yeast stress response through transitions between induced and constitutive activation. *Proc. Natl. Acad. Sci. U.S.A.* **108**, 16693–16698 (2011).
4. U. Schibler, F. Sierra, Alternative promoters in developmental gene expression. *Annu. Rev. Genet.* **21**, 237–257 (1987).
5. R. V. Davuluri, Y. Suzuki, S. Sugano, C. Plass, T. H. Huang, The functional consequences of alternative promoter use in mammalian genomes. *Trends Genet.* **24**, 167–177 (2008).
6. B. Tian, J. L. Manley, Alternative polyadenylation of mRNA precursors. *Nat. Rev. Mol. Cell. Biol.* **18**, 18–30 (2017).
7. S. Naftelberg, I. E. Schor, G. Ast, A. R. Kornblihtt, Regulation of alternative splicing through coupling with transcription and chromatin structure. *Annu. Rev. Biochem.* **84**, 165–198 (2015).
8. Y. Lee, D. C. Rio, Mechanisms and regulation of alternative pre-mRNA splicing. *Annu. Rev. Biochem.* **84**, 291–323 (2015).
9. J. V. Geisberg, Z. Moqtaderi, K. Struhl, The transcriptional elongation rate regulates alternative polyadenylation in yeast. *Elife* **9**, e59810 (2020).
10. F. Ozsolak *et al.*, Comprehensive polyadenylation site maps in yeast and human reveal pervasive alternative polyadenylation. *Cell* **143**, 1018–1029 (2010).
11. V. Pelechano, W. Wei, L. M. Steinmetz, Extensive transcriptional heterogeneity revealed by isoform profiling. *Nature* **497**, 127–131 (2013).
12. Z. Moqtaderi, J. V. Geisberg, Y. Jin, X. Fan, K. Struhl, Species-specific factors mediate extensive heterogeneity of mRNA 3′ ends in yeasts. *Proc. Natl. Acad. Sci. U.S.A.* **110**, 11073–11078 (2013).
13. J. V. Geisberg, Z. Moqtaderi, X. Fan, F. Ozsolak, K. Struhl, Global analysis of mRNA isoform half-lives reveals stabilizing and destabilizing elements in yeast. *Cell* **156**, 812–824 (2014).
14. Z. Moqtaderi, J. V. Geisberg, K. Struhl, Extensive structural differences of closely related 3′ mRNA isoforms: Links to Pab1 binding and mRNA stability. *Mol. Cell* **72**, 849–861 (2018).
15. S. N. Floor, J. A. Doudna, Tunable protein synthesis by transcript isoforms in human cells. *Elife* **5**, e10921 (2016).
16. C. Mayr, Evolution and biological roles of alternative 3′UTRs. *Trends Cell Biol.* **26**, 227–237 (2016).
17. H. Haruki, J. Nishikawa, U. K. Laemmli, The anchor-away technique: Rapid, conditional establishment of yeast mutant phenotypes. *Mol. Cell* **31**, 925–932 (2008).
18. V. Iyer, K. Struhl, Absolute mRNA levels and transcriptional initiation rates in *Saccharomyces cerevisiae*. *Proc. Natl. Acad. Sci. U.S.A.* **93**, 5208–5212 (1996).
19. M. D. Young, M. J. Wakefield, G. K. Smyth, A. Oshlack, Gene ontology analysis for RNA-seq: Accounting for selection bias. *Genome Biol.* **11**, R14 (2010).
20. Z. Moqtaderi, J. V. Geisberg, K. Struhl, A compensatory link between cleavage/polyadenylation and mRNA turnover regulates steady-state mRNA levels in yeast. *Proc. Natl. Acad. Sci. U.S.A.* **119**, e2121488119 (2022).
21. K. H. Lui, J. V. Geisberg, Z. Moqtaderi, K. Struhl, 3′ untranslated regions are modular entities that determine polyadenylation profiles. *Mol. Cell. Biol.* **42**, e0024422 (2022).
22. M. W. Webster, J. A. Stowell, L. A. Passmore, RNA-binding proteins distinguish between similar sequence motifs to promote targeted deadenylation by Ccr4-Not. *Elife* **8**, e40670 (2019).
23. B. Molinie *et al.*, m(6)A-LAIC-seq reveals the census and complexity of the m(6)A epitranscriptome. *Nat. Methods* **13**, 692–698 (2016).
24. I. J. Viegas *et al.*, N(6)-methyladenosine in poly(A) tails stabilize VSG transcripts. *Nature* **604**, 362–370 (2022).
25. X. Fan *et al.*, Nucleosome depletion in yeast terminator regions is not intrinsic and can occur by a transcriptional mechanism linked to 3′ end formation. *Proc. Natl. Acad. Sci. U.S.A.* **107**, 17945–17950 (2010).
26. Y. Jin *et al.*, Mapping 3′ mRNA isoforms on a genomic scale. *Curr. Protoc. Mol. Biol.* **110**, 4.23.1–4.23.17 (2015).
27. J. V. Geisberg *et al.*, Nucleotide-level linkage of transcriptional elongation and polyadenylation. *Elife* **11**, e83153 (2022).
28. R. Edgar, M. Domrachev, A. E. Lash, Gene Expression Omnibus: NCBI gene expression and hybridization array data repository. *Nucleic Acids Res.* **30**, 207–210 (2002).
29. J. V. Geisberg, Z. Moqtaderi, K. Struhl, Condition-specific 3′ mRNA isoform half-lives and stability elements in yeast. Gene Expression Omnibus. www.ncbi.nlm.nih.gov/geo/query/acc.cgi?acc=GSE228123. Deposited 24 March 2023.
30. Z. Moqtaderi, J. V. Geisberg, K. Struhl, Extensive structural differences of closely related 3′ mRNA isoforms: links to Pab1 binding and mRNA stability. Gene Expression Omnibus. www.ncbi.nlm.nih.gov/geo/query/acc.cgi?acc=GSE95788. Deposited 7 March 2017.
31. Z. Moqtaderi, J. V. Geisberg, K. Struhl, A compensatory link between cleavage/polyadenylation and mRNA turnover regulates steady-state mRNA levels in yeast. Gene Expression Omnibus. www.ncbi.nlm.nih.gov/geo/query/acc.cgi?acc=GSE191091. Deposited 16 December 2021.
32. J. V. Geisberg, Z. Moqtaderi, X. Fan, F. Ozsolak, K. Struhl, Global analysis of mRNA isoform half-lives: identification of stabilizing and destabilizing elements in yeast. Gene Expression Omnibus. www.ncbi.nlm.nih.gov/geo/query/acc.cgi?acc=GSE52286. Deposited 12 November 2013.